A Lumped-Circuit Model of the Two-Level Atom: Eigenstate Resonators, an Environment-Gated Radiative Channel, and the Origin of Spontaneous Emission

Derrick Hiang Yaol Lim*[1]

[1]Natureverse Thailand

Abstract

We present a classical, lumped-element circuit model of a two-level atom built around a specific conceptual claim: the two atomic energy eigenstates, represented as LC resonators with parameters fixed from the level energy and orbital magnetic moment, are *exactly* decoupled under the field-free Hamiltonian, which we realize as a literal open circuit between them. Coupling arises only from two distinct, independently gated perturbations: (i) an external oscillating field, modeled as a voltage source applied across the (otherwise open) inter-level branch, which produces reversible Rabi (continuous-wave drive) or Rosen–Zener (pulsed drive) dynamics; and (ii) the availability of a radiative channel in the environment – schematically, a receptive absorber elsewhere in the universe – modeled as a resistive path to a shared radiative bath that opens and closes in time, which produces irreversible photon emission via a shared-bath coupled-mode-theory (Haus) formalism. In the absence of both perturbations the model predicts, exactly, that an isolated excited atom does not radiate. We show the emission channel comes in two dual circuit realizations, inductive (magnetic-dipole, M1) and capacitive (electric-dipole, E1) coupling to the environment, and validate both against the hydrogen 21 cm hyperfine line and the Lyman-α ($2p \to 1s$) transition, reproducing the measured decay rates to within 1% and 0.2% respectively. We discuss the relationship of the "no absorber, no emission" baseline to Wheeler–Feynman absorber theory, to Cramer and Mead's two-atom transactional formalism, and to the standard vacuum-fluctuation picture.

1 Introduction

Consider a universe containing nothing but a single two-level atom, initialized in its excited state, with no other matter and no cavity modes to reflect or resonantly enhance any field the atom might produce. Does it radiate?

The question sounds like it should have an obvious answer, and in the standard treatment it does: the quantized electromagnetic field has vacuum fluctuations everywhere, always, regardless of what else is or is not present, and the atom's coupling to those vacuum modes is what drives spontaneous emission in the Wigner–Weisskopf treatment [2]. But the question has a second, less standard history. Wheeler and Feynman's absorber theory [7] and later discussions by Milonni [8] of the respective roles of vacuum fluctuations and radiation reaction in spontaneous emission both, in different ways, raise the possibility that emission is not solely a local property of the emitter – that a receptive absorber somewhere in the universe is doing more physical work than the vacuum-fluctuation picture alone suggests. More recently, Cramer and Mead [9] developed this

*Correspondence: natureverseth@gmail.com

absorber-dependent picture into an explicit two-atom quantum formalism: the electromagnetic coupling between an excited (emitter) hydrogen atom and a nearby ground-state (absorber) hydrogen atom factors into a matched retarded/advanced Green's-function pair whose combination uniquely enforces energy conservation, and the resulting dynamics – an initially small exchange between the two atoms that avalanches to the complete transfer of one photon's worth of energy – was proposed as a mechanism for wave-function collapse using ordinary Schrödinger mechanics alone, with no additional formalism required. We do not attempt to adjudicate any of this here. Instead, we use the underlying idea – that emission is not solely a local property of the emitter – as the organizing premise for a toy model: a lumped circuit in which the coupling that produces spontaneous emission is switched on explicitly, by an explicit "is a radiative channel available" variable, rather than being present unconditionally.

This paper builds that model in a self-contained way, organized around the two independent mechanisms by which the otherwise-decoupled eigenstates can interact. Section 2 sets up the circuit baseline: two LC resonators representing the atom's energy eigenstates, exactly decoupled by default. Section 3 treats the first mechanism, an external drive, together with its numerical results: the reversible Rabi and Rosen–Zener dynamics it produces. Section 4 treats the second mechanism, an environment-gated radiative channel, together with the correspondence-principle mapping (magnetic-dipole M1 and electric-dipole E1) needed to give it concrete atomic parameters, its numerical results, and its validation against the hydrogen 21 cm hyperfine line and Lyman-α. Section 5 discusses the model's relationship to the standard picture and its limitations, and Section 6 concludes.

2 Circuit Representation of Atomic Eigenstates: The Baseline

We represent each atomic energy eigenstate $|n\rangle$ (energy $E_n = \hbar\omega_n$) as an LC resonator storing one quantum of energy as a persistent current or charge oscillation, with L_n, C_n fixed from ω_n and the level's orbital magnetic (or electric transition) dipole moment by a correspondence-principle mapping (Sec. 4.2).

The key structural claim is this: because $|1\rangle$ and $|2\rangle$ are eigenstates of the atomic Hamiltonian H_0, they diagonalize it exactly, $\langle 1|H_0|2\rangle = 0$, by definition – not approximately, not "very weakly," but exactly. There is no term in H_0 alone that can move population from $|2\rangle$ to $|1\rangle$. The circuit realization of this fact is direct: *the branch connecting resonator 1 and resonator 2 is a literal open circuit, $Y(t) \equiv 0$, whenever no perturbation is present.* Figure 1 shows this baseline topology. There is no third, permanently-present "weak" coupling element sitting in that branch – the branch simply does not conduct until something is added to H_0.

Two, and only two, physical mechanisms can add a nonzero perturbation term $H'(t)$ on top of H_0, and we build a separate circuit mechanism for each, treated in turn in the next two sections:

- An **external field** (Sec. 3.1): a classical oscillating field applied to the atom, $H'(t) = -\boldsymbol{\mu} \cdot \mathbf{B}_{\text{ext}}(t)$ (M1) or $-\mathbf{d} \cdot \mathbf{E}_{\text{ext}}(t)$ (E1). This is reversible – it conserves the atom's total energy plus the field's, and, absent dissipation, produces coherent (Rabi or Rosen–Zener) population oscillation.

- An **available radiative channel** (Sec. 4.1): coupling to a continuum of environment modes, which can only carry energy *away* irreversibly if a receptive continuum – schematically, an absorber – exists to receive it. We gate this on and off explicitly as a stand-in for "is such an absorber available."

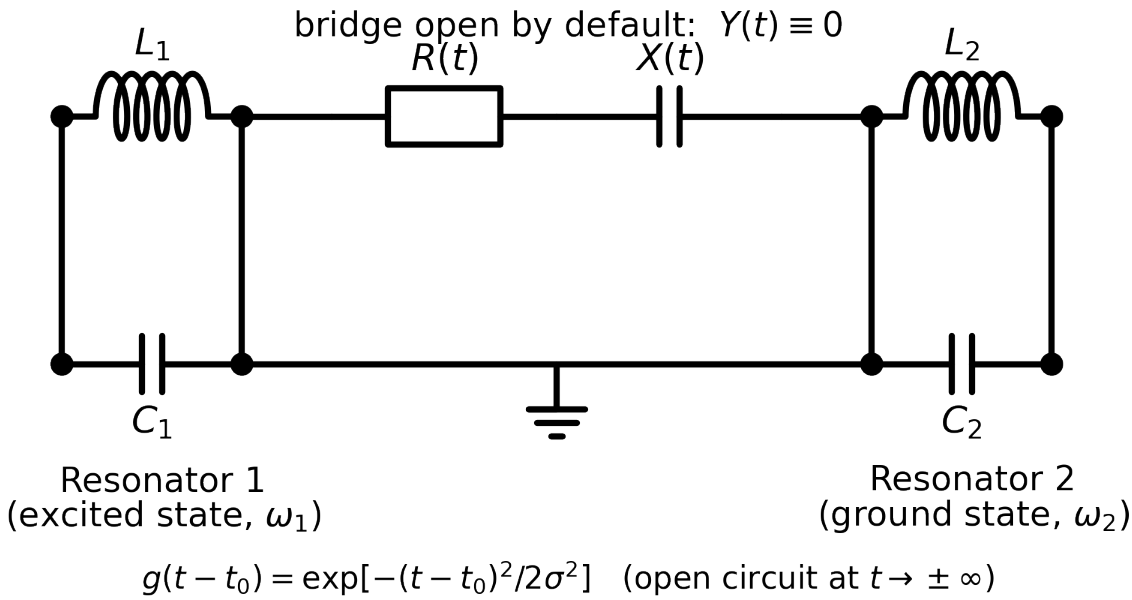

Figure 1: Baseline circuit topology: two parallel LC resonators representing the atom's excited and ground energy eigenstates. The bridge admittance $Y(t)$ is exactly zero – an open circuit – except while a perturbation (an external drive, Sec. 3.1, or an environment-gated radiative channel, Sec. 4.1) is present.

With neither mechanism present, $Y(t) \equiv 0$ for all time, the two resonators evolve independently, and a persistent current initialized in resonator 1 remains there *exactly*, for all time. In this toy model, an isolated excited atom with no external field and no available radiative channel does not radiate. This is not a numerical result requiring integration – it is the exact, algebraic content of the baseline model – but it is the paper's central claim, and both numerical sections below (Secs. 3.2 and 4.5) confirm it as their own starting point.

3 Driven Dynamics: Rabi and Rosen–Zener

3.1 Theory

To drive population between the two eigenstates without any dissipation, we add an oscillating voltage source $V_{\text{ext}}(t)$ in parallel across the (otherwise open) coupling branch, in series with a fixed reactance X_0 set by the same transition dipole moment (μ or d) that fixes the resonator parameters in Sec. 4.2 (Fig. 2). This is the circuit realization of the standard semiclassical dipole-field interaction: the strength with which an external field drives the transition is set by the very same matrix element that sets the resonator inductance/capacitance and (Sec. 4.1) the radiation resistance. One physical quantity, three roles.

Writing the envelope amplitudes as $a_1(t), a_2(t)$ (rotating-wave/slowly-varying-envelope approximation, $|a_j|^2 \propto$ stored energy), the driven, dissipation-free equations are

$$\dot{a}_1 = -i\kappa_{\text{drive}}(t)\, a_2\, e^{-i\Delta t}, \qquad \dot{a}_2 = -i\kappa_{\text{drive}}(t)\, a_1\, e^{+i\Delta t}, \tag{1}$$

with $\Delta = \omega_1 - \omega_2$ the transition frequency and $\kappa_{\text{drive}}(t) \propto \mu B_0(t)/\hbar$ or $dE_0(t)/\hbar$ the drive-induced coupling rate. Equation (1) conserves $|a_1|^2 + |a_2|^2$ exactly: with no radiative channel open, no

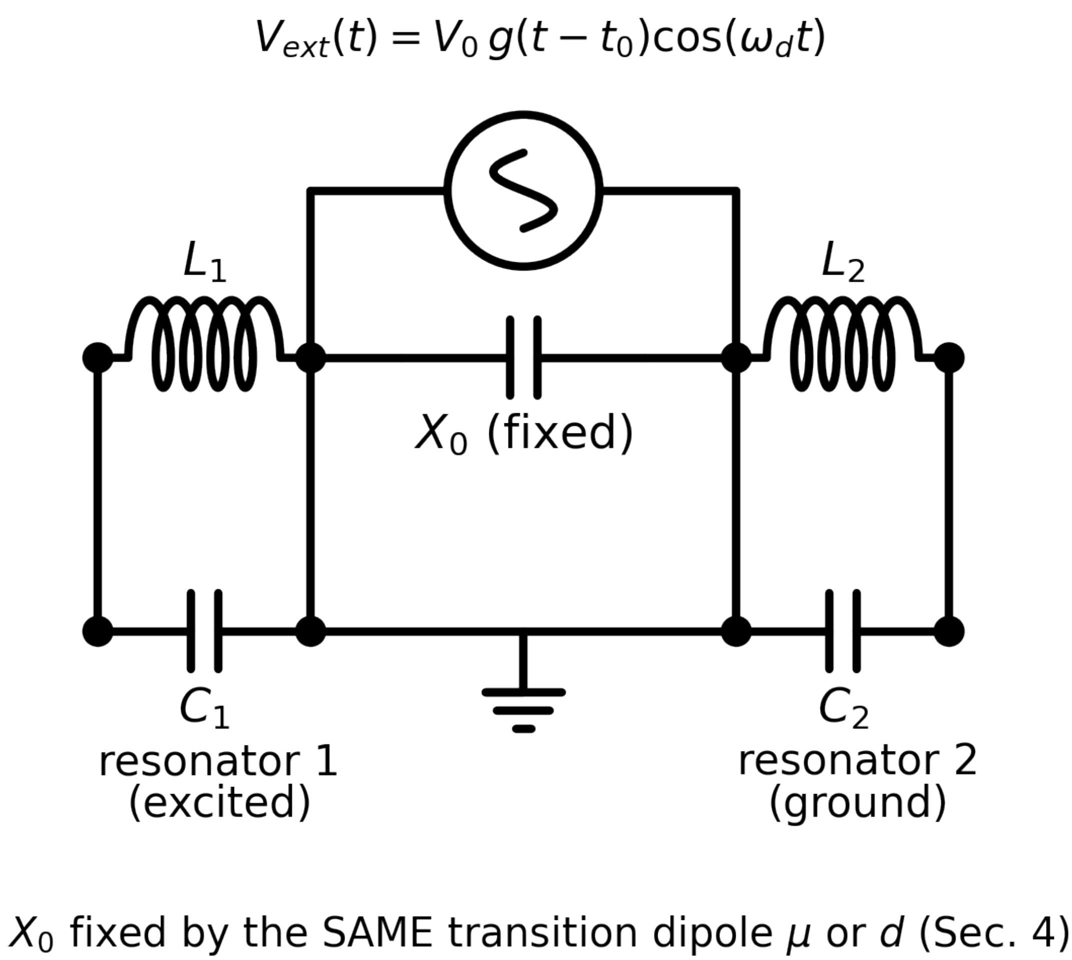

Figure 2: Stimulated-dynamics circuit: an external oscillating voltage source $V_{\text{ext}}(t) = V_0\, g(t - t_0)\cos(\omega_d t)$ is applied across the coupling branch. With no radiative channel present, this produces purely reversible dynamics – Rabi oscillation for a continuous-wave drive, Rosen–Zener population transfer for a pulsed drive.

photon is emitted by this mechanism, no matter how strong the drive – it only exchanges excitation coherently between the two resonators, exactly the classical analog of vacuum Rabi oscillation in strongly-coupled cavity QED, not of spontaneous emission.

Continuous-wave drive: Rabi oscillation. For a drive at exact resonance, $\omega_d = \Delta$, with constant envelope $g(t) \equiv 1$, the carrier-frequency rotating-wave reduction of the physical (lab-frame) drive $V_{\text{ext}}(t) = V_0 \cos(\omega_d t)$ leaves a time-independent effective coupling $\kappa_{\text{drive}} = \Omega_R/2$, and Eq. (1) integrates exactly, for $a_1(0) = 1, a_2(0) = 0$, to

$$a_1(t) = \cos(\Omega_R t/2), \qquad a_2(t) = -i\sin(\Omega_R t/2), \qquad N_2(t) = \sin^2(\Omega_R t/2), \tag{2}$$

the textbook Rabi formula, with Rabi frequency $\Omega_R = \mu B_0/\hbar$ (M1) or $dE_0/\hbar$ (E1) – undamped, exact, and periodic for as long as the drive is applied and no radiative channel is open. We confirmed Eq. (2) against direct numerical integration of Eq. (1), finding agreement to machine precision ($< 2 \times 10^{-15}$).

Pulsed drive: Rosen–Zener dynamics. For a drive envelope that turns on and off smoothly, $\kappa_{\text{drive}}(t) = \kappa_0\, g(t - t_0)$ with g a Gaussian or sech profile, Eq. (1) is precisely the Rosen–Zener two-level problem [1]: a fixed detuning Δ with a pulsed, non-crossing coupling. For a sech-shaped drive the exact transition probability is

$$P_{1\to 2}(\infty) = \left[\frac{\sin\Theta}{\cosh(\pi\Delta\tau/2)}\right]^2, \qquad \Theta \equiv \int_{-\infty}^{\infty} \kappa_{\text{drive}}(t)\, dt, \tag{3}$$

where Θ is the drive *pulse area*. No closed form exists for a Gaussian drive envelope, but the same qualitative structure survives, and we confirm it numerically next.

3.2 Numerical Results

With $\kappa_{\text{drive}}(t) \equiv 0$ (Sec. 2), Eq. (1) reduces immediately to $\dot{a}_1 = \dot{a}_2 = 0$: $a_1(t) = a_1(-\infty)$, $a_2(t) = 0$ for all time, identically – the exact baseline confirmed. Equation (2) (continuous-wave, on-resonance drive) was confirmed against direct numerical integration of Eq. (1) to machine precision, as noted above. For a pulsed drive, the equations were integrated numerically (adaptive Runge–Kutta, RK45, relative tolerance 10^{-8}) with $\gamma_j(t) \equiv 0$ (no radiative channel open – purely driven dynamics), $a_1(-\infty) = 1, a_2(-\infty) = 0$, and $\kappa_{\text{drive}}(t) = \kappa_{\text{peak}}\, g(t - t_0)$ with κ_{peak} chosen to realize a specified drive pulse area $\Theta = \int \kappa_{\text{drive}}\, dt$, using representative parameters $\Delta = 8.925 \times 10^9$ rad/s, $L_1 = L_2 = 4.235 \times 10^{-19}$ H corresponding to the hydrogen 21 cm transition (derived in Sec. 4.2 and 4.6 below).

Figure 3(a) sweeps the dimensionless pulse width $\sigma\Delta$ at fixed pulse area $\Theta = \pi/2$: population transfer to resonator 2 is efficient only for $\sigma\Delta \lesssim 1$ and is exponentially suppressed for slower (more adiabatic) drive pulses, confirming the qualitative prediction of Eq. (3). Figure 3(b) sweeps the pulse area Θ at fixed $\sigma\Delta = 0.3$: the population transfer follows an oscillatory (Rosen–Zener) fringe pattern, reaching near-complete transfer ($N_2 \approx 0.90$–0.94) near $\Theta = \pi/2$ and $3\pi/2$, and returning to near-zero transfer at $\Theta = \pi, 2\pi$ – the pulsed-drive analog of over-driving a Rabi π-pulse into a 2π pulse. Figure 3(c) shows an example time trace: the persistent current in resonator 1 decays smoothly (in an error-function-like envelope) as the drive pulse passes, transferring population almost entirely into resonator 2. Throughout this section $\gamma_j \equiv 0$, so, consistent with Sec. 3.1, the transfer is exactly reversible and no energy leaves the two-resonator system.

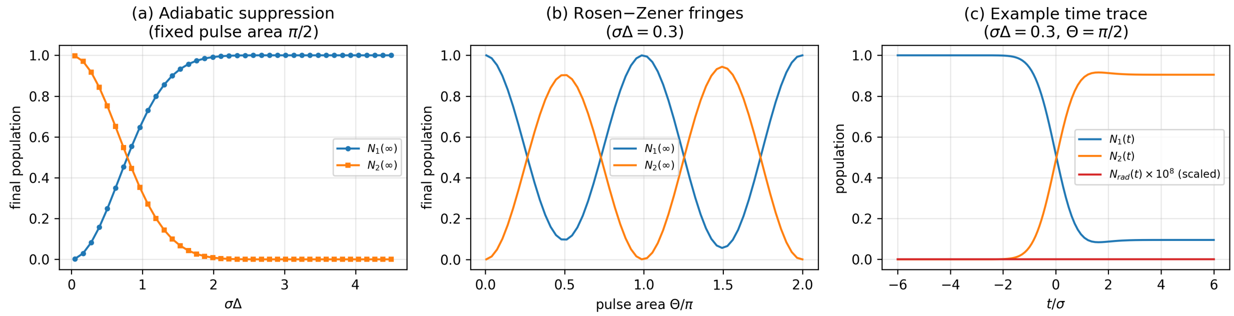

Figure 3: Driven dynamics with no radiative channel open [Eq. (1)], parametrized by the hydrogen 21 cm transition frequencies (Table 1). (a) Final populations vs. dimensionless drive-pulse width $\sigma\Delta$ at fixed pulse area $\Theta = \pi/2$. (b) Final populations vs. drive pulse area Θ at fixed $\sigma\Delta = 0.3$, showing Rosen–Zener fringes. (c) Example time trace at $\sigma\Delta = 0.3$, $\Theta = \pi/2$; the small labeled N_{rad} trace shows the (here, artificially retained for comparison) radiative loss if a channel matched to the physical R_{rad} of Table 1 were simultaneously left open (this radiative addition previewed from Sec. 4.1, not otherwise used in this figure).

4 Spontaneous Emission: The M1/E1 Radiative Channel

4.1 Theory: the environment-gated radiative channel

Genuine irreversibility requires coupling to a continuum, and specifically to a continuum with somewhere for the energy to go. The Wigner–Weisskopf result that a single discrete state coupled to only one other discrete state merely oscillates (Sec. 3.1) has a direct circuit analog: a bridge that only ever connects resonator 1 linearly to resonator 2, however it is engineered, cannot produce irreversible decay. We therefore let each resonator couple *separately* to a common radiative branch of instantaneous resistance $R(t)$, representing the free-space/environment channel, gated so that $R(t) \to 0$ (the branch is open – no receptive channel available) except while a window function $g(t - t_0)$ is nonzero, during which $R(t)$ rises toward the free-space impedance $Z_0 = 377\,\Omega$. We use this gate as an explicit stand-in for "a radiative channel – schematically, an absorbing atom or molecule elsewhere in the environment, in a matched-antenna-transmission sense – becomes available."

Because power is quadratic in current, a current $i_{\mathrm{rad}} = k_1 i_1 + k_2 i_2$ shared by both resonators automatically produces a cross (beat) term at exactly the transition frequency $\Delta = \omega_1 - \omega_2$ – the frequency of the physical photon – even though neither resonator individually oscillates there. Formalizing this via Haus coupled-mode theory [3] with a shared bath (the classical analog of Dicke collective/super-radiant damping [4]) gives, including both mechanisms together,

$$\dot{a}_1 = -\gamma_1(t)\,a_1 - i\kappa_{\mathrm{drive}}(t)\,a_2 e^{-i\Delta t} - \sqrt{\gamma_1(t)\gamma_2(t)}\;a_2 e^{-i\Delta t}, \tag{4}$$

$$\dot{a}_2 = -\gamma_2(t)\,a_2 - i\kappa_{\mathrm{drive}}(t)\,a_1 e^{+i\Delta t} - \sqrt{\gamma_1(t)\gamma_2(t)}\;a_1 e^{+i\Delta t}, \tag{5}$$

with $\gamma_j(t) = \frac{1}{2}R(t)/L_j$ the instantaneous radiative loss rate of resonator j into the shared bridge, and the outgoing radiated wave

$$s_{\mathrm{out}}(t) = \sqrt{2\gamma_1(t)}\,a_1(t) + \sqrt{2\gamma_2(t)}\,a_2(t). \tag{6}$$

Equations (4)–(6) conserve total energy exactly:

$$\frac{d}{dt}\left(|a_1|^2 + |a_2|^2\right) = -|s_{\mathrm{out}}(t)|^2, \tag{7}$$

which follows directly by substitution (κ_{drive} is purely reactive and drops out of the energy balance entirely; only the resistive terms contribute). This is the circuit-level statement of the Manley–Rowe / photon energy-conservation identity $\hbar\omega_1 = \hbar\omega_2 + \hbar\Delta$: one quantum leaves resonator 1, one quantum (at the lower energy) may appear in resonator 2, and the energy difference $\hbar\Delta$ is radiated. Figure 4 shows the full coupling topology schematically, with $\kappa_{\text{drive}}(t)$ and $\gamma_j(t)$ drawn as the two independent, separately gated mechanisms discussed above.

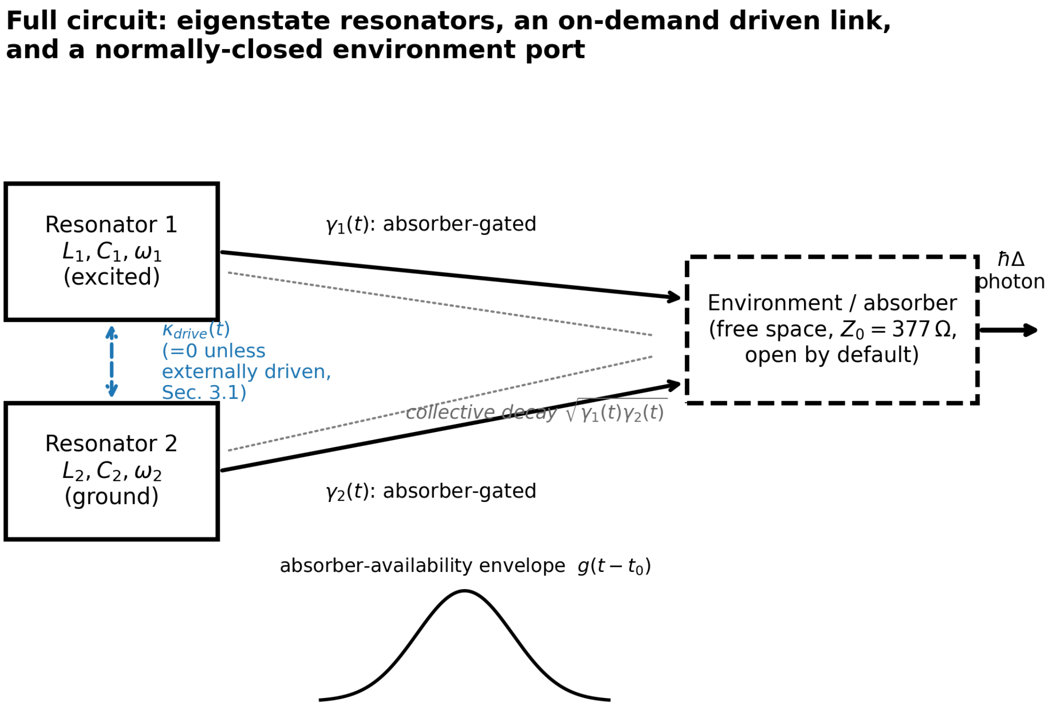

Figure 4: Full coupled-mode-theory representation of Eqs. (4)–(6). The direct link between the resonators is nonzero only while an external field drives $\kappa_{\text{drive}}(t)$ (Sec. 3.1, reversible). The link to the environment is nonzero only while a radiative channel is available, gating $\gamma_1(t), \gamma_2(t)$ (this section, irreversible), which automatically produces a collective cross-decay term $\sqrt{\gamma_1(t)\gamma_2(t)}$ and emits a photon at exactly $\hbar\Delta$.

For a single, isolated, permanently-matched resonator ($\gamma_1 \equiv \Gamma/2$ constant, no second resonator, no drive), Eq. (4) reduces to simple exponential energy decay $E_1(t) = E_1(0)e^{-\Gamma t}$ with

$$\Gamma = \frac{R_{\text{rad}}}{L_1}, \tag{8}$$

which we identify below as the classical statement of Fermi's Golden Rule – but note that even this simplest case requires $R_{\text{rad}} \neq 0$, i.e., an available channel; it does not happen "on its own."

4.2 Magnetic-dipole (M1) resonators

For a transition with orbital magnetic moment μ and energy $\hbar\omega_0$, we model the current as circulating around a loop of area A_{loop} (Fig. 5a). Matching the classical stored energy to one quantum and the classical peak magnetic moment to twice the quantum matrix element (the standard classical/quantum correspondence factor),

$$I_0 = \frac{2\mu}{A_{\rm loop}}, \qquad L = \frac{2\hbar\omega_0}{I_0^2}, \qquad C = \frac{1}{\omega_0^2 L}. \tag{9}$$

The small-loop radiation resistance $R_{\rm rad} = \mu_0\omega_0^4 A_{\rm loop}^2/(6\pi c^3)$ then gives, via Eq. (8),

$$\Gamma_{\rm M1} = \frac{\mu_0\,\omega_0^3\,\mu^2}{3\pi\hbar c^3}, \tag{10}$$

independent of the arbitrary loop-area choice, and identical to the textbook magnetic-dipole spontaneous-emission rate. The same μ fixes the Rabi frequency $\Omega_R = \mu B_0/\hbar$ of Sec. 3.1.

4.3 Electric-dipole (E1) resonators

For an E1 transition the radiating element must be a linear, oscillating charge dipole, not a loop (Fig. 5b). With physical charge-separation length l, dipole moment amplitude $p_0 = 2d$ (d the quantum transition dipole matrix element), and "antenna current" $I_0 = p_0\omega_0/l$,

$$L = \frac{2\hbar l^2}{p_0^2\omega_0}, \qquad R_{\rm rad} = \frac{\eta_0(k_0 l)^2}{6\pi} \quad (k_0 = \omega_0/c,\ \eta_0 = 1/\epsilon_0 c = 377\,\Omega), \tag{11}$$

which again gives an l-independent rate,

$$\Gamma_{\rm E1} = \frac{\omega_0^3\,d^2}{3\pi\epsilon_0\hbar c^3}, \tag{12}$$

exactly the textbook Einstein-A (electric-dipole) formula, with Rabi frequency $\Omega_R = dE_0/\hbar$. Because $\mu \sim e\omega_0 A_{\rm loop} \sim eva_0$ while $d \sim ea_0$, the M1 and E1 rates for atomic transitions of the same order of magnitude in geometric size differ by $(v/c)^2 \sim \alpha^2$, reproducing the well-known relative suppression of magnetic-dipole transitions in atomic physics.

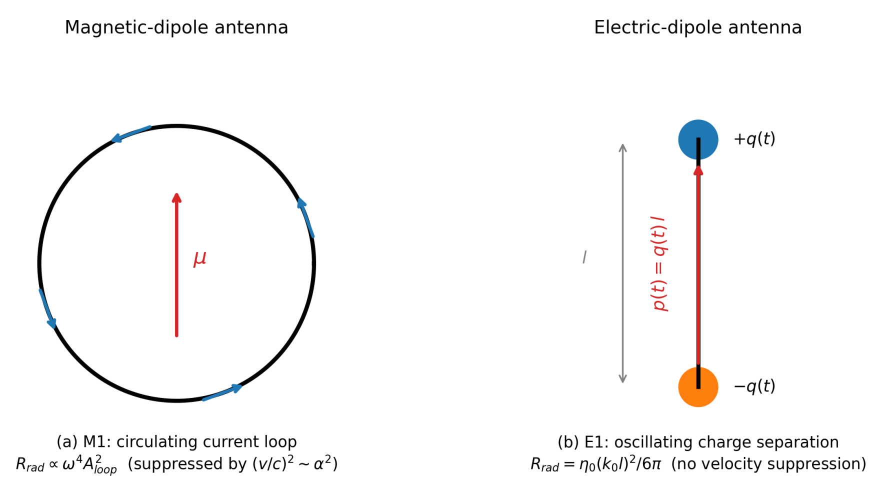

Figure 5: The two atomic radiator types realized in the circuit model. (a) A circulating persistent current (magnetic dipole, M1); radiation resistance is suppressed by the orbital velocity $(v/c)^2 \sim \alpha^2$. (b) An oscillating charge separation (electric dipole, E1); no such suppression is present.

4.4 Two radiative channels: inductive versus capacitive coupling to the environment

Secs. 4.2–4.3 fixed *what variable* each resonator stores its quantum in: an M1 resonator stores it as circulating current, an E1 resonator stores it as charge displacement. This choice fixes, uniquely, what *kind* of reactive element realizes both the driven coupling of Sec. 3.1 and the near-field coupling into the radiative channel of Sec. 4.1, by the standard electrostatic/magnetostatic duality of circuit theory ($L \leftrightarrow C$, current $\leftrightarrow$ charge, flux linkage $\leftrightarrow$ electric elastance):

M1: the coupling acts on *current*, so it is realized as a (driven or environment-gated) **mutual inductance**, entering the mesh (KVL) equations through the flux linkage $\Phi_1 = L_1 i_1 + M(t) i_2$:

$$L_1\ddot{q}_1 + M(t)\ddot{q}_2 + \dot{M}(t)\dot{q}_2 + \frac{q_1}{C_1} = -R(t)\dot{q}_1, \qquad L_2\ddot{q}_2 + M(t)\ddot{q}_1 + \dot{M}(t)\dot{q}_1 + \frac{q_2}{C_2} = -R(t)\dot{q}_2. \tag{13}$$

E1: the coupling acts on *charge*, so it is realized as a (driven or environment-gated) **mutual (bridging) capacitance** $C_m(t)$, entering the mesh equations directly as a shared elastance term:

$$L_1\ddot{q}_1 + R(t)(\dot{q}_1 - \dot{q}_2) + \frac{q_1}{C_1} + \frac{q_1 - q_2}{C_m(t)} = 0, \qquad L_2\ddot{q}_2 - R(t)(\dot{q}_1 - \dot{q}_2) + \frac{q_2}{C_2} - \frac{q_1 - q_2}{C_m(t)} = 0. \tag{14}$$

Figure 6 shows the two realizations side by side. In both, $M(t)$ or $C_m(t)$ and $R(t)$ are zero together, by the argument of Sec. 2, except while one of the two perturbations of Secs. 3.1–4.1 is present; only the *kind* of reactance differs between the M1 and E1 cases, and it is the same choice in both the driven-Rabi/Rosen–Zener context and the spontaneous-emission context, since both trace back to the same underlying transition dipole.

Repeating the rotating-wave envelope reduction of Sec. 3.1 on the purely reactive part of Eq. (14) gives the E1 driven-coupling rate

$$\kappa_{\text{drive}}(t) = \frac{1}{2\omega_1 L_1 C_m(t)}, \tag{15}$$

to be compared directly with the M1 result obtained from Eq. (13) in the same approximation, $\kappa_{\text{drive}} = M(t)\omega_2/4L_1$ (Sec. 3.1). The two expressions are related by the expected reactance duality: the inductive coupling rate *grows* with frequency ($\kappa \propto M\omega$, since inductive reactance is ωL), while the capacitive coupling rate *falls* with frequency ($\kappa \propto 1/\omega C_m$, since capacitive reactance is $1/\omega C$).

4.5 Numerical results: detuning suppression and the vanishing-resistance limit

With the drive off ($\kappa_{\text{drive}} \equiv 0$) and the radiative channel gated by $\gamma_j(t) = \frac{1}{2}[R_{\text{peak}}/L_j]g(t - t_0)$, R_{peak} set to the physically correct R_{rad} of Secs. 4.2–4.3, the same numerical method as Sec. 3.2 gives the radiated-energy fractions reported below (Secs. 4.6–4.7). Because $R(t)$ is the only irreversible element in the model, exact "complete quenching" of resonator 1 ($N_1(\infty) = 0$) by the radiative channel alone generically requires strong exposure, $\Gamma_1\sigma \gg 1$ where $\Gamma_1 \equiv 2\gamma_{1,\text{peak}}\sigma\sqrt{2\pi}$; complete transfer can instead be reached, without any dissipation at all, via the driven Rosen–Zener resonance of Sec. 3.2. In the strict limit of vanishingly small (but positive) R_0, with a drive held fixed, the dissipative channel vanishes linearly in R_0 while the driven channel is unaffected; for any $R_0 > 0$, however small, a residual $O(R_0)$ fraction of the energy is unavoidably dissipated whenever the two mechanisms are simultaneously active, since the radiative branch necessarily carries some current during a driven swap.

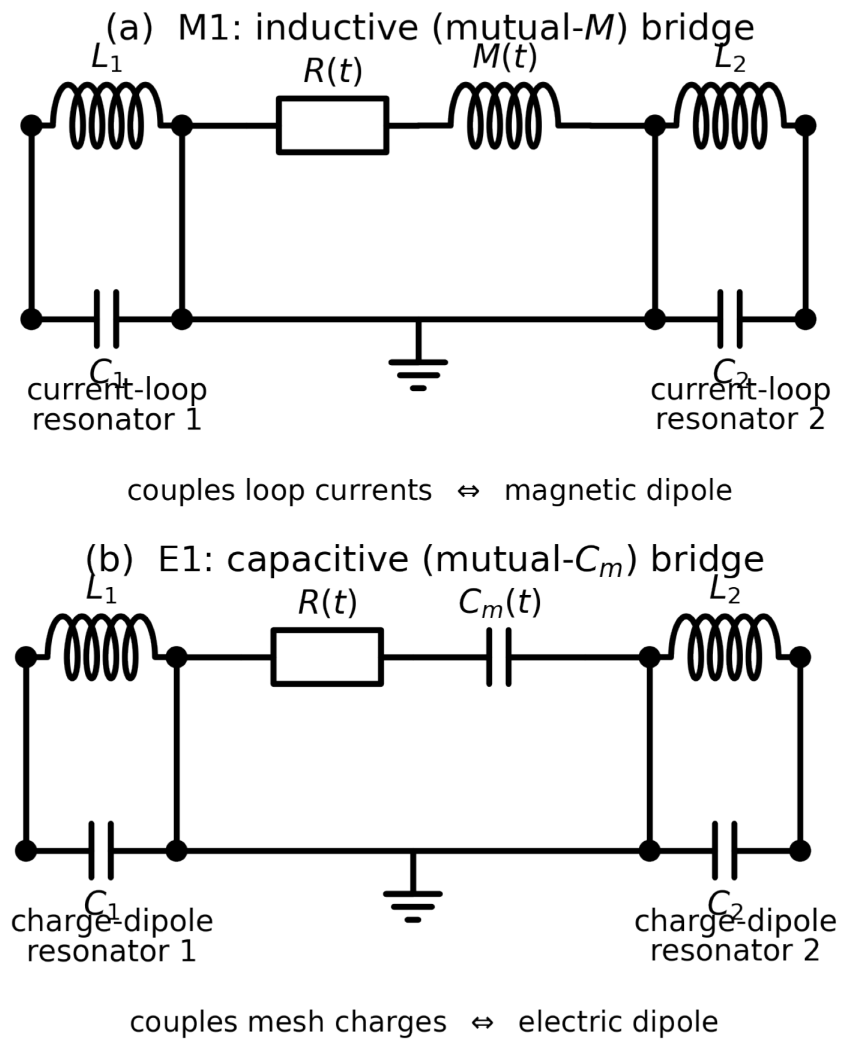

Figure 6: Electrical duality of the coupling reactance. (a) M1: two current-loop resonators coupled by a mutual inductance $M(t)$. (b) E1: two charge-dipole resonators coupled by a mutual capacitance $C_m(t)$. In both cases $R(t)$ plays the same role: the environment-gated approach to the free-space impedance match of Sec. 4.1.

4.6 Validation: hydrogen 21 cm hyperfine transition (M1)

Using $\omega_0 = \Delta = 2\pi \times 1420.405\,751\,\text{MHz}$, $\mu = \mu_B$, and $A_{\text{loop}} = \pi a_0^2$ in Eqs. (9)–(10) gives the parameters and result in Table 1. The predicted rate agrees with the measured Einstein coefficient $A_{10} = 2.85 \times 10^{-15}\,\text{s}^{-1}$ [5] to better than 1%. The physically self-consistent radiation resistance, $R_{\text{rad}} \approx 1.2 \times 10^{-33}\,\Omega$, is dramatically mismatched from the idealized free-space value of $377\,\Omega$ ($R_{\text{rad}}/Z_0 \sim 10^{-36}$), which is the circuit-level statement of why this transition is so extraordinarily slow – equivalently, of how rarely, in the environment-gated picture of Sec. 4.1, an effectively matched channel is on offer.

Table 1: Hydrogen 21 cm hyperfine transition: M1 circuit parameters and predicted decay rate.

Quantity	Value
$\omega_0 = \Delta$	8.925×10^9 rad/s
μ	μ_B
I_0	2.108×10^{-3} A
$L_1 = L_2$	4.235×10^{-19} H
$C_1 = C_2$	2.965×10^{-2} F
R_{rad} (physically self-consistent)	1.215×10^{-33} Ω
Γ_{M1} predicted [Eq. (10)]	2.869×10^{-15} s^{-1}
A_{10} measured [5]	2.850×10^{-15} s^{-1}
Ratio (predicted/measured)	**1.007**

4.7 Validation: hydrogen Lyman-α, $2p \to 1s$ (E1)

Table 2 compares the M1 (loop) and E1 (dipole) predictions for the $2p \to 1s$ transition ($\lambda = 121.567\,\text{nm}$). The M1 loop model, using the same procedure as for the hyperfine line, underestimates the measured rate by a factor of $\sim 2 \times 10^4$, consistent with the expected α^2 suppression for a transition that is genuinely electric-dipole in character. Rebuilding the resonator as an oscillating charge dipole [Eq. (11)], using the independently tabulated quantum dipole matrix element $d = 0.7449\,ea_0$ [6] (not fit to the measured rate), reproduces the measured Einstein coefficient $A_{21} = 6.265 \times 10^8\,\text{s}^{-1}$ [5] to within 0.2%.

Table 2: Hydrogen Lyman-α ($2p \to 1s$) transition: M1 vs. E1 circuit predictions.

Quantity	M1 (loop, incorrect)	E1 (dipole, correct)
Moment used	$\mu = \sqrt{2}\,\mu_B$	$d = 0.7449\,ea_0$
L	3.676×10^{-13} H	8.53×10^7 H[a]
R_{rad} (self-consistent, $l = a_0$)	1.10×10^{-8} Ω	1.50×10^{-4} Ω
Γ predicted	3.00×10^4 s^{-1}	6.258×10^8 s^{-1}
A_{21} measured [5]	6.265×10^8 s^{-1}	6.265×10^8 s^{-1}
Ratio (predicted/measured)	$\mathbf{4.79 \times 10^{-5}}$	**0.9989**

[a] Reported for the convention $l = 1$ m used to isolate the intrinsic, l-independent rate Γ; the physically meaningful, atomic-scale ($l = a_0$) circuit values are $L = 2.39 \times 10^{-13}$ H, $C = 1.74 \times 10^{-20}$ F, $I_0 = 3.70 \times 10^{-3}$ A.

5 Discussion

The central claim, and how it relates to the standard picture. The model's baseline prediction – no external field, no available radiative channel, no radiation – is a stronger and more specific statement than ordinary Wigner–Weisskopf theory makes, since the standard treatment couples the atom to the quantized vacuum field unconditionally, present or absent any receiving structure. Our environment-gating of $R(t)$ is closer in spirit to Wheeler–Feynman absorber theory [7], to Milonni's discussion [8] of the (in ordinary QED, formally equivalent, but conceptually distinct) roles of vacuum fluctuations versus radiation reaction in spontaneous emission, and to Cramer and Mead's two-atom transactional formalism [9], than to the mainstream vacuum-fluctuation account. The parallel to the latter is worth making explicit: in their treatment, the emitter and absorber atoms each develop a small oscillating admixture of the other's state, with dipole moments oscillating at exactly the same difference frequency $\omega_0 = \omega_2 - \omega_1$ – our Δ – and a correctly phase-matched exchange "avalanches" to the complete transfer of one photon's worth of energy. This is structurally the same picture as the pulse-area resonance of Sec. 3.1 (population transfer completing at $\Theta = \pi/2, 3\pi/2, \ldots$, and returning to near-zero away from those values) and the Manley–Rowe photon accounting of Sec. 4.1 ($\hbar\omega_1 = \hbar\omega_2 + \hbar\Delta$), even though we build it from classical circuit elements rather than a two-atom Schrödinger calculation. We want to be precise about what we are and are not claiming: we have not derived the absorber-dependence of emission from first-principles QED, and mainstream theory does not require an absorber for an isolated atom to radiate. What we have shown is that a simple, quantitatively accurate (Secs. 4.6–4.7) circuit model can be built on the alternative premise, and that doing so requires nothing exotic – just an explicit "is a channel available" gate rather than an always-on coupling. We offer this as a pedagogically useful toy, not as a claim about which picture is physically correct. We note in passing that the parenthetical restriction "barring any cavity modes" in the motivating question is itself physically loaded: were a cavity present, its modes would modify $R_{\mathrm{rad}}(\omega_0)$ (the Purcell effect [10]), which in our circuit picture is just a statement that the environment can be a better- or worse-matched channel depending on what is nearby – consistent with, and a natural quantitative extension of, the gating idea itself.

Limitations. First, the correspondence-principle factor of 2 relating classical peak moments to quantum matrix elements, and the choice of atomic-scale geometric parameters ($A_{\mathrm{loop}} = \pi a_0^2$, $l = a_0$), are standard but not unique conventions; because the final rates $\Gamma_{\mathrm{M1}}, \Gamma_{\mathrm{E1}}$ are independent of these geometric choices [Eqs. (10),(12)], the validated results do not depend on this arbitrariness, but the intermediate circuit component values (L, C, and especially R_{rad}) do. Second, the model is a mean-field, classical amplitude theory and does not capture quantum fluctuation statistics (e.g., photon antibunching) without further, genuinely quantum, input. Third, our lumped single-resistor bath is the Markovian, flat-spectral-density limiting case of a true continuum, exact only insofar as the relevant bandwidth ($\sim \sigma^{-1}$) is much smaller than the range over which the free-space impedance may be treated as frequency-independent, which is well satisfied for both transitions studied here. Finally, the finite-pulse ("instantaneous matching") construction of Sec. 4.1 naturally produces a single-shot, non-exponential (error-function) energy-loss profile rather than a continuous exponential decay law; recovering the latter requires treating many independent, randomly-timed channel-availability events as a Poisson process, whose ensemble-averaged rate converges to Γ – a natural and, we believe, physically instructive constructive derivation of Fermi's Golden Rule that we leave for future work.

6 Conclusion

The toy circuit model presented here is, in a precise sense, semi-empirical: its linear building blocks – LC resonators for the eigenstates, a driven bridge for stimulated transitions, a shared resistive bath for spontaneous emission – are all standard, textbook circuit elements, and all of the model's non-trivial dynamics come from a single, deliberately non-linear ingredient: a coupling admittance that switches in time according to the state of the atom's environment (whether an external field is present, whether a radiative channel is available), not according to any internal property of the atom alone. Once that switching is specified, everything else – Rabi oscillation, Rosen–Zener fringes, and Fermi's-Golden-Rule spontaneous emission at rates matching the hydrogen 21 cm and Lyman-α lines to 1% and 0.2% – follows from ordinary, linear circuit theory. We think this makes the model useful less as a computational tool than as an explanatory one: it offers a concrete, buildable, quantitatively checkable picture of why an excited atom's fate depends on what else exists to receive its energy, and a simple analogy for introducing Rabi oscillation, Rosen–Zener dynamics, and spontaneous emission together, from one small set of circuit elements, in an educational setting.

References

[1] N. Rosen and C. Zener, "Double Stern-Gerlach Experiment and Related Collision Phenomena," *Phys. Rev.* **40**, 502 (1932).

[2] V. Weisskopf and E. Wigner, "Berechnung der natürlichen Linienbreite auf Grund der Diracschen Lichttheorie," *Z. Phys.* **63**, 54 (1930).

[3] H. A. Haus, *Waves and Fields in Optoelectronics* (Prentice-Hall, 1984).

[4] R. H. Dicke, "Coherence in Spontaneous Radiation Processes," *Phys. Rev.* **93**, 99 (1954).

[5] A. Kramida, Yu. Ralchenko, J. Reader, and NIST ASD Team, *NIST Atomic Spectra Database* (ver. 5.11), National Institute of Standards and Technology, Gaithersburg, MD.

[6] H. A. Bethe and E. E. Salpeter, *Quantum Mechanics of One- and Two-Electron Atoms* (Springer, 1957).

[7] J. A. Wheeler and R. P. Feynman, "Interaction with the Absorber as the Mechanism of Radiation," *Rev. Mod. Phys.* **17**, 157 (1945).

[8] P. W. Milonni, *The Quantum Vacuum: An Introduction to Quantum Electrodynamics* (Academic Press, 1994).

[9] J. G. Cramer and C. A. Mead, "Symmetry, Transactions, and the Mechanism of Wave Function Collapse," *Symmetry* **12**, 1373 (2020).

[10] E. M. Purcell, "Spontaneous Emission Probabilities at Radio Frequencies," *Phys. Rev.* **69**, 681 (1946).